3P5-23

Proceedings of Symposium on Ultrasonic Electronics, Vol. 34 (2013) pp. 535-536
20-22 November, 2013

Measurement of shear wave propagation in elasticity phantom considering phase fluctuation of echo signals

スペックルによる位相変動の影響を考慮した生体擬似ファントム内の横波伝搬計測

Hirofumi Sasaki[1†], Shinnosuke Hirata[1], and Hiroyuki Hachiya[1] ([1]Tokyo Inst. of Tech.)
佐々木日史[1†]，平田慎之介[1]，蜂屋弘之[1]([1]東工大)

1. Introduction

It is known that the shear modulus of the fibrotic liver tissues becomes larger than that of the normal tissues. Many approaches to evaluate the degeneration degree of liver by generating shear wave in tissues have been proposed. However, the method using acoustic radiation force to generate shear wave has potential to produce bio-effects on human tissues. So it is desired to improve measurement sensitivity of the shear wave. In this study, we generated shear wave in phantom and considered about accurate measurement method of its displacement. By synchronizing the timing of shear wave generation and diagnostic pulse wave transmission, we got 2-D images of shear wave displacement which has no effects of beam scan time. Next, we reduced measurement error caused by phase fluctuation of echo signals and present possibility of more accurate measurement.

2. Measurement of shear wave displacement in phantom

We generated shear wave in the phantom by the acoustic radiation force of focused ultrasound generated by concave transducer. The focused ultrasound is a burst wave of 2.3 MHz sine-wave signal and its duration is about 20 ms. As shown in Fig. 1, a phantom that contains four spheres whose shear modulus is different from background was used. After shear wave was generated, we got echo signals from the phantom successively by the single transducer. As shown in Fig. 2, from 40 ms later after shear wave generation, we transmitted diagnostic pulse wave (frequency 10 MHz) 6 times in a row by interval of 10 ms and got its echo signals. Next, we scanned the transducer about 27.5 mm at interval of 0.185 mm. At each position of transducer, we generated shear wave in the same way and transmitted pulse wave at the same delay time after shear wave generation. In this way, we got B-mode images of phantom which has no time lag for lateral direction.

In this study, we calculated the shear wave displacement by phase difference of echo signals. First, we demodulated the i^{th}echo signal of one scan line and got its initial phase $\phi_i(d)$ where d is the depth. Next, we calculated phase difference between $\phi_i(d)$ and $\phi_{i+1}(d)$. Then we converted it to the axial displacement Δx from the equation

$$\Delta x_i(d) = \frac{\lambda \Delta \phi_i(d)}{4\pi}, \qquad (1)$$

where λ is wave length of pulse wave in the water. Positive Δx means downward displacement of shear wave and negative Δx means upward displacement. By applying this method to all scan lines, we got 2-D plot of shear wave displacement.

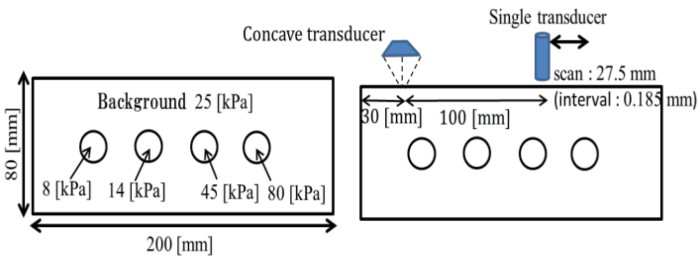

Fig. 1 Experiment configuration

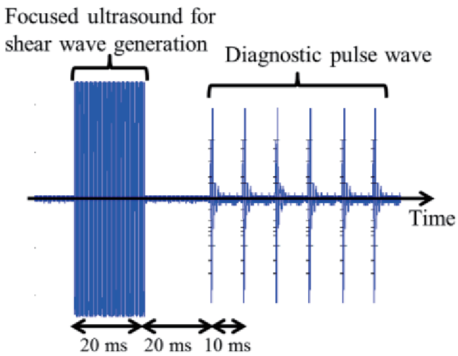

Fig. 2 shear wave generation and pulse echo

3. Results and discussion

Fig. 3 shows 2-D plot of axial displacement. t means elapsed time from the beginning of shear wave generation. The maximum axial displacement is about 10 μm and it is about 1/10 of the ultrasound wave length. Eliminating the effects of beam scan time, we visualized shear wave front with the small displacement. Next, we considered about the measurement errors. When the echo signal from phantom is expressed by $A(t)\sin(\omega_0 t + \phi(t))$, it is known that initial phase $\phi(t)$ fluctuates for depth direction. As shown in Fig. 4, when the phantom displaces Δx for depth direction between i^{th} and

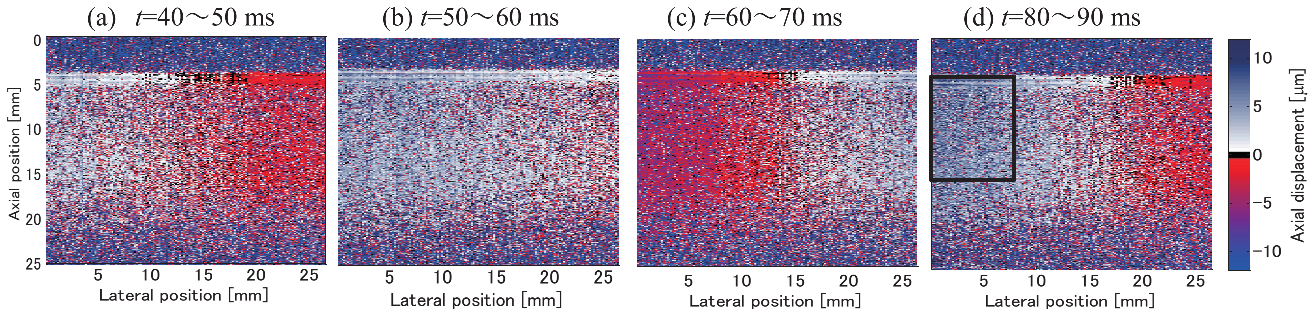

Fig. 3 2-D plot of axial displacement

$(i+1)^{th}$ echo signals, time shift Δt is caused between the two signals. Then, initial phase of $(i+1)^{th}$ echo signal is expressed by $\phi(t-\Delta t)+\Delta\phi$ where $\Delta\phi$ is theoretical phase difference corresponding to Δx. As a result, phase difference is measured $\Delta\phi_m(t)=\phi(t-\Delta t)+\Delta\phi-\phi(t)$ and measurement error is caused by phase fluctuation. Values of the measurement error rely on Δx and $q(t)$ expressed by dotted line in Fig. 4. $q(t)$ corresponds to instantaneous frequency variation $\Delta\omega(t)$ which is expressed by $\Delta\omega(t)=\omega(t)-\omega_0$ where $\omega(t)$ is instantaneous frequency. These relations are expressed by the equation

$$\Delta\phi_m(t)=\frac{2\Delta x(2\pi f-\Delta\omega(t))}{c} \qquad (2)$$

where c is ultrasound speed in the water.

In Fig. 3 (d), we showed region of interest (ROI) by square in which displacement appears to be relatively stable. Average displacement in ROI is 4.44 μm. Fig. 5(a) shows the relation between instantaneous frequency and measured displacement in ROI. The horizontal axis means the value of $\Delta\omega(t)$ and the vertical axis means the value of $\Delta x_m(t)$. Colorbar shows the mapping of numbers to colors. The displacement measurement value is affected by the value of $\Delta\omega(t)$. As a result, measurement error is caused. To reduce the error, we estimated $\Delta x(t)$ from measured $\Delta\omega(t)$ and $\Delta\phi_m(t)$ using Eq. (2). Fig. 5(b) shows the histogram of estimated $\Delta x(t)$ in ROI. The vertical axis means corrected $\Delta x(t)$. Standard deviation of displacement in ROI is reduced from 5.88 μm to 4.45 μm. Figure 6 shows the comparison between images in ROI before and after error reduction .We found that accurate measurement is possible by reducing the effects of instantaneous frequency fluctuation.

4. Conclusion

We measured shear wave displacement less than 10 μm by initial phase of echo signals and visualized shear wave front which has no time lag for lateral direction. Moreover, we applied the method to reduce measurement error caused by the instantaneous frequency fluctuation of echo signals and indicated the possibility of more accurate measurement.

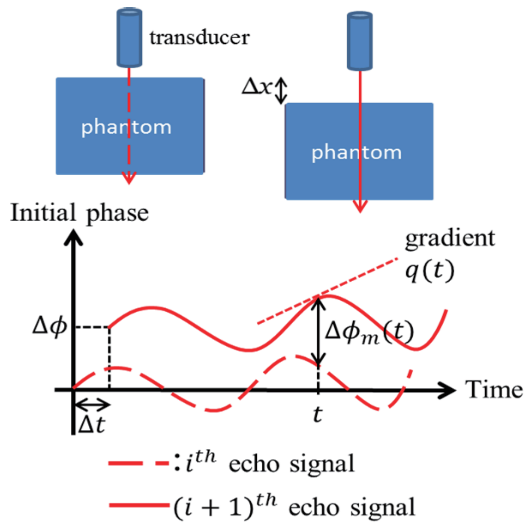

Fig. 4 Measurement error cause of axial displacement

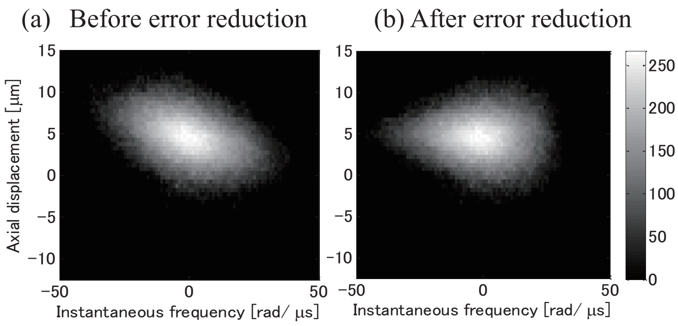

Fig. 5 Instantaneous frequency and measured displacement

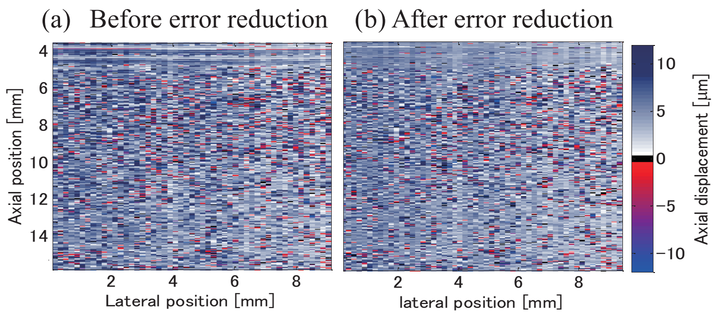

Fig. 6 2-D plot of axial displacement in the ROI

References

1. M.Yamakawa: Jpn. J. Appl. Phys. Vol.40, 2001; 3872.
2. T.Shiina: J Med Ultrasonics Vol.29, 2002; 119.